

Advancing Security and Sustainability in Cost-Effective Multi-Band Flexible-Grid Optical Networks: Optimization Models and Algorithms

Ibrahima Diarrasouba
Le Havre Normandie University,
LMAH, FR CNRS 3335
76600 Le Havre, France
diarrasi@univ-lehavre.fr

Youssef Hadhbi*
Orange Research
92320 Châtillon, France
youssef.hadhbi@orange.com

A. Ridha Mahjoub
Department of Statistics and
Operations Research, College of
Science, Kuwait University
Kuwait
ridha.mahjoub@ku.edu.kw

Abstract

In the context of evolving optical communication networks, ensuring security and cost-effectiveness while maintaining high performance and energy efficiency is of critical importance. This paper proposes an optimization framework for multi-band elastic optical networks (MB-EONs) that integrates resilience, security levels, and energy efficiency for each traffic demand by avoiding vulnerable nodes and links susceptible to cyberattacks and failures. Focusing on the Routing, Modulation, Spectrum, and Band Assignment, key issues for the operation of MB-EONs, we initially develop two ILP models: one based on a cut formulation and the other on an extended formulation. Due to the high number of variables in the extended model, we employ a column generation algorithm to solve its linear relaxation. Based on these results, we design two exact algorithms based on Branch-and-Cut and Branch-and-Price algorithms. Numerical experiments across diverse instances, examining their behavior, and complemented by a comparative study identifying the most effective algorithm for solving the problem.

Keywords

EON, Multi-Band Networks, SDM, Resilience, Security, Energy, ILP, Column Generation, Branch-and-Cut, Branch-and-Price.

1 Introduction

The exponential growth of global data traffic, driven by the extensive use of mobile devices, digital services, and the deployment of advanced wireless technologies such as 5G and the upcoming 6G networks, poses significant challenges for telecommunication infrastructures [7]. In response to this, optical networks have advanced into flexible and scalable architectures referred to as Elastic Optical Networks (EONs) or FlexGrid networks. These networks utilize adaptable spectrum slices, supporting higher data rates, dynamic bandwidth allocation, and more efficient resource utilization. Recently, a new architecture called Multi-band EONs has been proposed [17], which utilizes multiple frequency bands within the optical spectrum (such as O, C, L, S, and E bands), enabling the simultaneous transmission of data across these bands. This approach significantly enhances spectral efficiency by making better use of the available spectrum and allows for flexible resource allocation tailored to varying traffic demands [23]. Additionally, MB-EONs are generally easier to implement compared to space division multiplexing (SDM) EONs, which rely on the

spatial separation of signals through multiple fibers or cores [17]. SDM systems often involve higher CAPEX costs, complex hardware, and more intricate management, making multi-band EONs a more practical and scalable solution for increasing network capacity. As a consequence, multi-band EONs are considered a more attractive technology for supporting the high data rates, low latency, and diverse service requirements of next-generation networks [23].

This paper proposes optimization models and algorithms specifically designed to enhance the performance and efficiency of multi-band EONs. Our focus is on enhancing MB-EON planning within a combinatorial optimization framework that integrates critical aspects such as security, resilience, and energy efficiency. By incorporating these considerations into our models, we aim to identify optimal strategies for resource allocation and routing, thereby improving the overall performance and sustainability of MB-EONs. Addressing these interconnected challenges is crucial for developing optical networks that are secure, resilient, and environmentally sustainable.

In this context, this paper addresses the Routing, Modulation, Spectrum, and Band Assignment (RMSBA) problem for controlling multi-band elastic optical networks. This involves optimizing traffic routing, bandwidth allocation, and modulation formats across multiple frequency bands to maximize spectral efficiency. Key constraints include spectrum continuity, contiguity, avoiding overlaps, and respecting transmission reach limits dictated by modulation choices. Additionally, the complexity increases with the need to coordinate spectrum allocation across multiple bands, ensuring efficient utilization while minimizing interference. Compared to the traditional NP-hard Routing and Spectrum Assignment (RSA) problem [24] which has been extensively studied in the literature [2], the RMSBA problem is more recent and complex, as it involves additional subproblems such as modulation format selection and band assignment [25]. Selecting the appropriate modulation format for each demand depends on various factors like transmission distance, bandwidth needs, and network topology. The inclusion of band assignment further increases the complexity of RMSBA compared to the Routing, Modulation and Spectrum Assignment (RMSA) alone [17][25]. Regarding network resilience, numerous survivability schemes have been proposed to enhance capacity [20] and robustness while ensuring service continuity under failure scenarios [13][21]. Some of these techniques have been applied to the RMSBA problem using heuristic methods [23], and AI [14][15]. Additionally, recent studies have explored sustainable solutions for MB-EONs [9][16] and various security mechanisms to protect network integrity [22].

To the best of our knowledge, the simultaneous consideration of

*Corresponding author.

INOC '26, Liège (Belgium)

© 2026 Copyright held by the owner/author(s). Published on OpenProceedings.org under ISBN 978-3-89318-105-6, series ISSN 2510-7437. Distribution of this paper is permitted under the terms of the Creative Commons license CC-by-nc-nd 4.0.

resilience, security, and sustainability in cost-effective RMSBA has not yet been explored in the literature. Additionally, polyhedral approaches and decomposition methods have not been applied to the RMSBA, even when these aspects are not considered. These approaches have proven effective for the RSA problem in [4–6, 12] and for the Routing Wavelength Assignment (RWA) in [3]. Therefore, this paper introduces the first optimization framework for RMSBA that integrates resilience, security, and energy considerations, utilizing *column generation* and *cutting-plane* algorithms. Our mathematical models are based on two integer linear programming formulations: the first, referred to as the *cut formulation*, and the second, an extended formulation referred to as the *path formulation*, which involves a significantly larger number of variables. To deal with this, we develop a column generation algorithm to solve the linear relaxation of the extended formulation and investigate its associated pricing problem. Based on these results, we develop two exact optimization approaches: a *Branch-and-Cut* (B&C) algorithm based on the cut formulation, and a *Branch-and-Price* (B&P) algorithm based on the path formulation. We evaluate their effectiveness through a series of computational experiments and perform a comparative analysis to assess their performance, scalability, and suitability for solving problems of different sizes and complexities. The rest of this paper is organized as follows. The RMSBA problem is described in Section 2. In Section 3, we introduce the cut formulation of the RMSBA problem and develop a Branch-and-Cut algorithm to solve it. Section 4 presents the path formulation and details the column generation approach used to solve its linear relaxation. A Branch-and-Price algorithm is then developed to solve the problem. Section 5 provides a presentation of the computational results, including performance analysis and comparative study between our approaches. Finally, Section 6 concludes the paper with a summary of results and discusses potential directions for future research.

2 Problem Description

The RMSBA problem can be modeled as follows. The topology of the MB-EON network is represented by an undirected, loopless, and connected graph $G = (V, E)$, where V is the set of nodes (such as data centers, core routers, or edge devices), and E is the set of fiber links. Each link $e \in E$ is characterized by its length $\ell_e \in \mathbb{R}^+$ (in kms), cost c_e (in euros), and a subset of spectrum bands $B_e \subseteq \{C, L, S, E\}$. These bands are defined as spectrum slots: $\mathbb{S}^C = \{1, \dots, \bar{s}_C\}$, $\mathbb{S}^L = \{1, \dots, \bar{s}_L\}$, $\mathbb{S}^E = \{1, \dots, \bar{s}_E\}$, and $\mathbb{S}^S = \{1, \dots, \bar{s}_S\}$. The overall spectrum set is $\mathbb{S} = \{1, \dots, \bar{s}\}$, where $\bar{s} = \max\{\bar{s}_C, \bar{s}_L, \bar{s}_S, \bar{s}_E\}$.

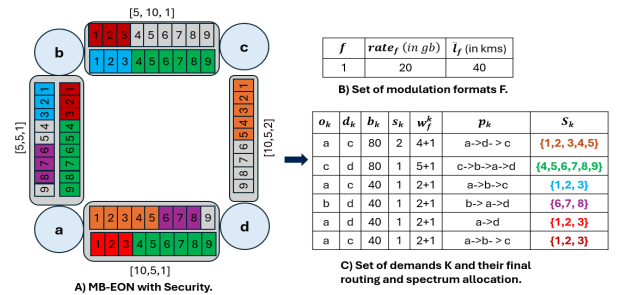
The network must serve a set of non-splittable traffic demands K , where each demand $k \in K$ is characterized by its origin node $o_k \in V$, destination node $d_k \in V$, and bandwidth requirement b_k (in Gbps). Regarding security, several key parameters are taken into account: the security level of each demand, denoted as s_k , can take values in $\{1, 2, 3\}$, representing increasing levels of security from basic protection to highly secure transmission. The vulnerability of each node $i \in V$, denoted as v_i , assesses its susceptibility to attacks or failures, with $v_i \in \{0, 1, 2\}$ (0: low vulnerability, 1: moderate, 2: high). Similarly, the vulnerability of links, v_e , is evaluated within $\{0, 1, 2\}$, with the same interpretation. Based on this, we denote by V_0^k the set of nodes $i \in V \setminus \{o_k, d_k\}$ such that $v_i > s_k$, referred to as forbidden nodes due to security constraints. Also, we denote by E_0^k the set of edges $e \in E$ with $v_e > s_k$, also considered forbidden edges due to security constraints. This means

that even highly vulnerable nodes or links can be used for highly secure requests, as long as their vulnerability does not exceed the security level required. In addition, a set of modulation formats \mathcal{F} is considered. Each modulation format $f \in \mathcal{F}$ is characterized by its spectral efficiency η_f (in Gbps per slot) and its maximum reach $\bar{\ell}_f$ (in kms), which is the maximum transmission distance achievable without regeneration.

The RMSBA involves selecting one routing path p_k , choosing one modulation format $f_k \in \mathcal{F}$, and allocating one spectrum interval $S_k \subset \mathbb{S}$ for each demand $k \in K$. These allocations must satisfy several physical and operational constraints. First, the total spectrum width $w_{f_k}^k$ allocated to demand k must be sufficient to meet its bandwidth requirement b_k , calculated as: $w_{f_k}^k = \left\lceil \frac{b_k}{\eta_{f_k} \cdot B} \right\rceil + 1$, where $B = 12.5$ GHz is the bandwidth per slot [21]. The additional slot accounts for a guard band to prevent interference between adjacent spectrum allocations. Also, the spectrum S_k for each demand must be allocated across a band $b \in B_e$ on each link e in the path p_k , maintaining spectrum continuity. The total length of the path p_k must satisfy the maximum reach constraint associated with the selected modulation format: $\sum_{e \in p_k} \ell_e \leq \bar{\ell}_{f_k}$. Furthermore, the selected path must avoid nodes and links with vulnerability levels exceeding the demand's security level s_k , ensuring both security and resilience. Specifically, it cannot pass through nodes V_0^k and links E_0^k , as these vulnerability values are indicative of both security risks and failure. Spectrum continuity must be preserved along the entire path. For this, the spectrum S_k allocated to demand k must be contiguous and consistent throughout p_k , with no gaps. Spectrum contiguity also requires that the allocated spectrum intervals are contiguous blocks within \mathbb{S} . Notice that allocations for different demands k and k' must not overlap on shared bands over the same link. The total number of slots used on each band $b \in B_e$ of each link e to all demands passing through it must not exceed the available spectrum \bar{s}_b . Regarding energy consumption, each active slot consumes a fixed amount of energy, E_{slot} (in Watts). The total energy used is estimated by multiplying the number of active slots in each band by E_{slot} , summed across all bands used in the network. Additionally, a maximum energy consumption \bar{E}_{Green} is considered to promote energy-efficient and green network operation for the MB-EONs. The main goal is to minimize the total routing cost of all demands, ensuring an efficient, reliable, and cost-effective network operation for MB-EONs.

Figure 1 illustrates a feasible solution to the RMSBA problem, involving six demands, a single modulation format, and at most two bands allocated per link. Each link is characterized by a triplet (ℓ_e, c_e, v_e) , and each node $i \in V$ has vulnerability $v_i = 0$.

Figure 1: A feasible solution for an instance of the RMSBA.



In the following sections, we devise two exact optimization approaches to solve the RMSBA problem.

3 Branch-and-Cut Algorithm

The first approach employs a Branch-and-Cut algorithm to solve the RMSBA problem. For this, we first introduce the cut formulation based on the following decision variables.

For each demand $k \in K$, each modulation format $f \in F$, and each spectrum slot $s \in S$, we consider the variable $z_{f,s}^k$ which is set to 1 if slot s is the last in the spectrum interval S_k allocated to demand k using modulation format f , and 0 otherwise. Additionally, for each demand $k \in K$, modulation format $f \in F$, slot $s \in S$, edge $e \in E$, and band $b \in B_e$, the binary variable $x_{f,s,b}^{k,e}$ is set to 1 if slot s is the last allocated to demand k over band b of edge e with modulation format f , and 0 otherwise. Furthermore, we define another binary variable $a_{b,s}^e$, which equals 1 if slot $s \in \mathbb{S}^b$ is utilized on band b of edge e , and 0 otherwise.

The RMSBA problem is then equivalent to solving the following linear program:

$$\sum_{e \in E} \sum_{b \in B_e} \sum_{f \in F} \sum_{s=w_f^k}^{\bar{s}_b} c_e \cdot x_{f,s,b}^{k,e}, \quad (1)$$

subject to

$$\sum_{e \in \delta(X)} \sum_{b \in B_e} \sum_{f \in F} \sum_{s=w_f^k}^{\bar{s}_b} x_{f,s,b}^{k,e} \geq 1, \quad \forall k \in K, \forall X \subset V: |X \cap \{o_k, d_k\}| = 1, \quad (2)$$

$$\sum_{f \in F} \sum_{s=w_f^k}^{\bar{s}} z_{f,s}^k = 1, \quad \forall k \in K, \quad (3)$$

$$\sum_{b \in B_e} x_{f,s,b}^{k,e} \leq z_{f,s}^k, \quad \forall k \in K, \forall e \in E, \forall f \in F, \forall s \in \{w_f^k, \dots, \bar{s}\}, \quad (4)$$

$$\sum_{e \in E} \sum_{b \in B_e} \sum_{s=w_f^k}^{\bar{s}} \ell_e \cdot x_{f,s,b}^{k,e} \leq \bar{\ell}_f \cdot \sum_{s=w_f^k}^{\bar{s}} z_{f,s}^k, \quad \forall k \in K, \forall f \in F, \quad (5)$$

$$\sum_{k \in K} \sum_{f \in F} \sum_{s'=s}^{\min(s+w_f^k-1, \bar{s}_b)} x_{f,s',b}^{k,e} \leq a_{b,s}^e, \quad \forall e \in E, \forall b \in B_e, \forall s \in \mathbb{S}^b, \quad (6)$$

$$\sum_{k \in K} \sum_{f \in F} \sum_{s=w_f^k}^{\bar{s}_b} w_f^k \cdot x_{f,s,b}^{k,e} \leq \bar{s}_b, \quad \forall e \in E, \forall b \in B_e, \quad (7)$$

$$\sum_{s=1}^{\bar{s}_b} a_{b,s}^e \geq \sum_{k \in K} \sum_{f \in F} \sum_{s=w_f^k}^{\bar{s}_b} w_f^k \cdot x_{f,s,b}^{k,e}, \quad \forall e \in E, \forall b \in B_e, \quad (8)$$

$$\sum_{e \in E} \sum_{b \in B_e} \sum_{s=1}^{\bar{s}_b} E_{slot} \cdot a_{b,s}^e \leq \bar{E}_{Green}, \quad (9)$$

$$\sum_{f \in F} \left[\sum_{s=1}^{w_f^k-1} z_{f,s}^k + \sum_{e \in E} \sum_{b \in B_e} x_{f,s,b}^{k,e} \right] = 0, \quad \forall k \in K, \quad (10)$$

$$\sum_{f \in F} \sum_{e \in E} \sum_{b \in B_e} \sum_{s=\bar{s}_b+1}^{\bar{s}} x_{f,s,b}^{k,e} = 0, \quad \forall k \in K, \quad (11)$$

$$\sum_{i \in V_0^k} \sum_{f \in F} \sum_{e \in \delta(i)} \sum_{b \in B_e} \sum_{s=1}^{\bar{s}_b} x_{f,s,b}^{k,e} = 0, \quad \forall k \in K, \quad (12)$$

$$\sum_{e \in E_0^k} \sum_{f \in F} \sum_{b \in B_e} \sum_{s=1}^{\bar{s}_b} x_{f,s,b}^{k,e} = 0, \quad \forall k \in K, \quad (13)$$

$$z_{f,s}^k \geq 0, \quad \forall k \in K, \forall f \in F, \forall s \in S, \quad (14)$$

$$x_{f,s,b}^{k,e} \geq 0, \quad \forall k \in K, \forall f \in F, \forall e \in E, \forall b \in B_e, \forall s \in \mathbb{S}^b, \quad (15)$$

$$0 \leq a_{b,s}^e \leq 1, \quad \forall e \in E, \forall b \in B_e, \forall s \in \mathbb{S}^b, \quad (16)$$

$$z_{f,s}^k \in \{0, 1\}, \quad \forall k \in K, \forall f \in F, \forall s \in S, \quad (17)$$

$$x_{f,s,b}^{k,e} \in \{0, 1\}, \quad \forall k \in K, \forall f \in F, \forall e \in E, \forall b \in B_e, \forall s \in \mathbb{S}^b. \quad (18)$$

The objective function (1) aims to minimize the total routing cost of demands. Inequalities (2), known as *cut inequalities*, ensure that the final path for each demand forms a continuous, feasible route from the source to the destination, respecting the network topology. These constraints prevent disjointed or infeasible paths. In addition, constraint (3) ensures that each demand is assigned exactly one modulation format for its entire route, establishing a consistent modulation choice along the path. Additionally, this constraint links the modulation assignment to spectrum allocation by guaranteeing that if a demand uses modulation format f , exactly one slot within the allowed range S_k is designated as the last slot, maintaining spectrum continuity along the route. Constraints (4) establish the relationship between the last-slot assignment, modulation format, and band assignment over edges, ensuring consistency and continuity in spectrum usage. Inequalities (5) restrict the total length of each demand's path to not exceed the maximum transmission distance supported by the chosen modulation format, ensuring feasible signal transmission. To prevent spectrum overlaps, inequalities (6) enforce non-overlapping spectrum allocations among different demands sharing the same band on each edge. The capacity constraints for each band on each edge are enforced by inequalities (7), which limit the total spectrum usage within available slots. These are further refined by inequalities (8), which specify the minimum number of slots required on each band $b \in B_e$ of every edge $e \in E$, ensuring sufficient spectrum for demand requirements.

The total energy consumption is constrained by inequalities (9), limiting the overall energy used by the network. Constraints (10) prevent the allocation of slots below the minimum ending position w_f^k , while constraints (11) ensure that the maximum ending position over each band is maintained within feasible limits. The security constraints are expressed through equations (12)-(13).

All decision variables are restricted within defined bounds by inequalities (14)–(16) when considering the linear relaxation of the model. Also, constraints (17)–(18) guarantee their binary nature. Note that the cut inequalities (2) are exponential in number. However, these inequalities are separable in polynomial time using network flow algorithms, like Goldberg and Tarjan algorithm [11]. The overall complexity of the separation procedure for these inequalities across all demands is bounded by $\mathcal{O}(|V|^2 \cdot \sqrt{|E|} \cdot |K|)$ [5]. Based on these results, we develop a Branch-and-Cut algorithm to solve the RMSBA problem. This integrates a *Branch-and-Bound* (B&B) with a cutting-plane algorithm, which iteratively refines the linear relaxation of the problem. Starting from an initial relaxed formulation (3)-(16), the algorithm identifies violated cut inequalities (2). These inequalities are then added dynamically as cutting planes to eliminate infeasible regions from the solution space, thereby tightening the feasible region and guiding the algorithm toward optimal solutions. This process repeats until no new cuts are found. The resulting solution is optimal for the linear relaxation. Moreover, if it is integral, it is optimal for the original problem. Otherwise, we branch on a fractional variable to create subproblems, continuing the process until an optimal integer solution is found.

Next, we introduce the path formulation, and devise a Branch-and-Price algorithm to solve the RMSBA problem.

4 Branch-and-Price Algorithm

The path formulation shares all the variables with the cut formulation. Additionally, we consider the path variables $u_{f,p}^k$, which take the value 1 if path $p \in P_{k,f}$ is used to route demand k when modulation format f is assigned to that demand, and 0 otherwise. Here, $P_{k,f}$ denotes the set of all (o_k, d_k) -paths where the length of each path $p \in P_{k,f}$ is less than $\bar{\ell}_f$. We denote by $P_{k,f}(e)$ the subset of paths in $P_{k,f}$ that pass through edge e . Moreover, this formulation shares all the constraints with the cut formulation, except for the cut inequalities (2), which are replaced by the following constraints:

$$\sum_{p \in P_{k,f}} u_{f,p}^k = \sum_{s=w_f^k}^{\bar{s}} z_{f,s}^k, \quad \forall k \in K, \forall f \in F, \quad (19)$$

$$\sum_{f \in F} \sum_{p \in P_{k,f}(e)} u_{f,p}^k \leq \sum_{b \in B_e} \sum_{f \in F} \sum_{s=w_f^k}^{\bar{s}_b} x_{f,s,b}^{k,e}, \quad \forall k \in K, \forall e \in E. \quad (20)$$

Inequalities (19) ensure that only one path is selected to route each demand, and that the chosen path is compatible with the assigned modulation format. In addition, inequalities (20) indicate whether, for demand k , the edge e is used in the final route or not.

As previously noted, the path formulation involves an exponential number of variables due to the potentially large number of feasible paths $|P_{k,f}|$ for each demand $k \in K$ and modulation format $f \in F$, meaning that $|P_{k,f}|$ can grow exponentially. To manage this, we develop a column generation algorithm to solve its linear relaxation. This begins with a restricted master problem (RMP) containing a small subset of path variables, which provides a feasible basis for the master problem. To initialize this set, we precompute a set of candidate paths $P_{k,f}^{init} \subseteq P_{k,f}^k$ for each demand k and modulation format f using a brute-force algorithm in a sub-graph $G_k = (V \setminus V_0^k, E \setminus E_0^k)$, while respecting the maximum length $\bar{\ell}_f$. The resulting set of paths forms a feasible initial basis for the RMP.

At each iteration, the algorithm checks for the existence of a variable $u_{f,p}^k$ not currently in the RMP with a negative reduced cost. If such a variable exists, it is added to the RMP, which is then resolved. The process terminates when all path variables u have non-negative reduced costs. The problem of identifying variables with negative reduced costs is known as the *pricing problem*. This involves finding a feasible path p for demand k and modulation format f such that the variable $u_{f,p}^k$ has a negative reduced cost, if such a path exists.

Let $\alpha_f^k \in \mathbb{R}$ and $\lambda_e^k \leq 0$ be the dual variables associated with the constraints (19) and (20) respectively. These dual variables are used to compute the reduced cost for potential paths that are not yet included in the current basis of the RMP. Based on this, the reduced cost of a path p for demand k and modulation format f is: $RC(p) = \alpha_f^k - \sum_{e \in p} \lambda_e^k$. The main goal is to identify, for each demand $k \in K$ and modulation format $f \in F$, a path p^* in $G_k = (V \setminus V_0^k, E \setminus E_0^k)$ with

$$RC(p^*) = \alpha_f^k - \min_{p \in P_{k,f}^k} \sum_{e \in p} \lambda_e^k < 0 \text{ subject to } \sum_{e \in p^*} \ell_e \leq \bar{\ell}_f. \quad (21)$$

The variable u_{f,p^*}^k corresponding to the path p^* with the most negative reduced cost can be added to the current RMP to enhance the solution. As a consequence, the pricing problem can be formulated as a *Resource Constrained Shortest Path Problem*, which is known to be weakly NP-hard [8]. For this, we propose a pseudo-polynomial time dynamic programming algorithm to solve it.

By integrating a Branch-and-Bound algorithm with column generation, we develop a Branch-and-Price algorithm to solve the RMSBA problem. In this approach, column generation is used to solve the linear relaxation at each node of the branching tree.

5 Computational Study

The Branch-and-Cut and Branch-and-Price algorithms were developed in C++ using SCIP 7.0 [10], while CPLEX 12.9 [18] served as the LP solver. Computational tests were conducted on a Debian GNU/Linux 9.13 system. The hardware setup included an Intel Xeon E5-2650 v2 processor with 32 cores running at 2.60 GHz, and a total RAM capacity of 248 GB. Each instance was allocated a maximum CPU time of 18000 seconds. The test instances comprised four realistic graphs from SND-LIB [19], and four from RSA-LIB [1], featuring up to 161 nodes and 166 edges as shown in Table 1.

Table 1: List of graphs used in the experiments.

Graphs		V	E	Average Degree
SND-LIB	German	17	25	2,94
	Nsfnet	14	21	3
	Brain	161	166	2,06
	France	25	45	3,6
RSA-LIB	British	22	35	3,18
	DT	14	23	3,29
	UBN	24	34	3,58
	Euro	16	36	4,5

For each graph, the demand set K was generated randomly, with $|K|$ taking values in $\{10, 20, 30, 40, 50, 100, 150, 200\}$.

For each demand set size $|K|$, four distinct demand sets were generated, resulting in a total of 32 instances per graph (total of 250 instances). The demand bandwidths b_k were uniformly distributed within the interval $[200, 400]$ Mbps. Additionally, three distinct modulation formats were used. When $|K| \leq 50$, only the C band was considered; for $100 \leq |K| \leq 150$, both C and L bands were employed; and for $|K| \geq 200$, three bands C, L, and S were utilized on each edge. The maximum number of slots for \bar{s}_C , \bar{s}_L , and \bar{s}_S reached up to 320. Regarding security and vulnerability parameters, we randomly assign security and vulnerability levels while maintaining demand routing feasibility. Similarly, for each band b , we verify that the allocated slots \bar{s}_b suffice to route all demands K .

The results of the B&C and B&P methods are summarized in Table 2. Several indicators are considered, based on the average across the four instances for each graph and value of $|K|$: the average number of nodes in the branching tree (AvgNd), the average optimality gap (AvgGap) for only instances that were solved (i.e., instances for which the solver provides at least a feasible primal solution), the average computational time (AvgTT), the number of instances solved to optimality (OPT), and the number of instances for which the solver failed to find a solution (NOSOL).

Table 2: Comparison between B&C and B&P algorithms.

Instance				Branch-and-Cut					Branch-and-Price				
Graph	K	Bands	S	AvgNd	AvgGap	#OPT	#NOSOL	AvgTT	AvgNd	AvgGap	#OPT	#NOSOL	AvgTT
German	10	C	80	1	0,00	4/4	0/4	23,05	1	0,00	4/4	0/4	67,20
	20	C	240	1	0,00	4/4	0/4	325,04	1	0,00	4/4	0/4	214,96
	30	C	320	1	0,00	4/4	0/4	4834,27	1	0,00	4/4	0/4	586,92
	40	C	320	1	0,00	3/4	1/4	15019,32	1	0,00	4/4	0/4	1085,49
	50	C	320	1	1,92	1/4	3/4	18000,00	1	0,00	4/4	0/4	2148,60
	100	C+L	320	1	-	0/4	4/4	18000,00	1	0,00	4/4	0/4	263,38
	150	C+L	320	1	-	0/4	4/4	18000,00	1	0,00	4/4	0/4	542,22
200	C+L+S	320	1	-	0/4	4/4	18000,00	1	0,00	3/4	1/4	4920,26	
Nsfnet	10	C	80	2,75	0,00	4/4	4/4	321,36	1	0,00	4/4	0/4	1,65
	20	C	320	733,75	8,83	1/4	2/4	16548,51	1	0,00	4/4	0/4	16,35
	30	C	320	1	-	0/4	4/4	18000,00	1	0,00	4/4	0/4	25,55
	40	C	320	1	-	0/4	4/4	18000,00	1	0,00	4/4	0/4	39,31
	50	C	320	1	-	0/4	4/4	18000,00	1	0,00	4/4	0/4	57,14
	100	C+L	320	1	-	0/4	4/4	18000,00	10,5	3,38	2/4	0/4	9583,55
	150	C+L	320	1	-	0/4	4/4	18000,00	1	9,53	0/4	2/4	18000,00
200	C+L+S	320	1	-	0/4	4/4	18000,00	2,5	15,42	0/4	3/4	18000,00	
Brain	10	C	160	705,75	0,00	1/4	3/4	13889,46	1	0,00	4/4	0/4	17,88
	20	C	160	1	-	0/4	4/4	18000,00	1	0,00	4/4	0/4	35,38
	30	C	160	1	-	0/4	4/4	18000,00	1	0,00	4/4	0/4	65,73
	40	C	160	1	-	0/4	4/4	18000,00	1	0,00	4/4	0/4	129,39
	50	C	200	1	-	0/4	4/4	18000,00	1	0,00	4/4	0/4	149,50
	100	C+L	320	1	-	0/4	4/4	18000,00	1	-	0/4	4/4	18000,00
	150	C+L	320	1	-	0/4	4/4	18000,00	1	-	0/4	4/4	18000,00
200	C+L+S	320	1	-	0/4	4/4	18000,00	1	-	0/4	4/4	18000,00	
France	10	C	160	1	0,00	4/4	0/4	147,42	1	0,00	4/4	0/4	50,11
	20	C	200	1	0,00	4/4	0/4	524,40	1	0,00	4/4	0/4	539,00
	30	C	200	1	0,00	1/4	3/4	17902,23	1	0,00	4/4	0/4	320,16
	40	C	200	1	-	0/4	4/4	18000,00	1	0,00	4/4	0/4	815,66
	50	C	240	1	-	0/4	4/4	18000,00	1	0,00	4/4	0/4	368,19
	100	C+L	320	1	-	0/4	4/4	18000,00	1	0,00	4/4	0/4	2313,12
	150	C+L	320	1	-	0/4	4/4	18000,00	1	-	0/4	4/4	18000,00
200	C+L+S	320	1	-	0/4	4/4	18000,00	1	0,00	4/4	0/4	5904,06	
British	10	C	80	1	0,00	4/4	0/4	28,89	1	0,00	4/4	0/4	5,28
	20	C	160	1	0,00	4/4	0/4	150,11	1	0,00	4/4	0/4	24,85
	30	C	160	1	0,00	4/4	0/4	5928,33	1	0,00	4/4	0/4	49,15
	40	C	240	1	-	0/4	4/4	18000,00	1	0,00	4/4	0/4	141,24
	50	C	240	1	-	0/4	4/4	18000,00	1	0,00	4/4	0/4	218,55
	100	C+L	320	1	-	0/4	4/4	18000,00	1	0,00	4/4	0/4	2723,65
	150	C+L	320	1	-	0/4	4/4	18000,00	2	0,00	4/4	0/4	10085,56
200	C+L+S	320	1	-	0/4	4/4	18000,00	1,5	0,78	3/4	0/4	11122,66	
DT	10	C	80	1	0,00	4/4	0/4	11,05	1	0,00	4/4	0/4	2,53
	20	C	160	1	0,00	4/4	0/4	43,41	1	0,00	4/4	0/4	12,87
	30	C	160	1	0,00	4/4	0/4	87,22	1	0,00	4/4	0/4	18,52
	40	C	240	1	0,00	3/4	1/4	9990,60	1	0,00	4/4	0/4	44,74
	50	C	240	1	-	0/4	4/4	18000,00	1	0,00	4/4	0/4	63,42
	100	C+L	320	1	-	0/4	4/4	18000,00	1	0,00	4/4	0/4	648,51
	150	C+L	320	1	-	0/4	4/4	18000,00	10,5	6,69	0/4	0/4	18000,00
200	C+L+S	320	1	-	0/4	4/4	18000,00	13,50	2,65	2/4	0/4	11272,71	
UBN	10	C	80	1	0,00	4/4	0/4	23,74	1	0,00	4/4	0/4	145,73
	20	C	160	1	0,00	4/4	0/4	103,44	1	0,00	4/4	0/4	833,40
	30	C	160	1	0,00	4/4	0/4	5208,44	1	0,00	4/4	0/4	1088,89
	40	C	240	1	0,00	3/4	1/4	11757,30	1	0,00	4/4	0/4	1296,32
	50	C	240	1	-	0/4	4/4	18000,00	1	0,00	4/4	0/4	1832,89
	100	C+L	320	1	-	0/4	4/4	18000,00	1	0,00	4/4	0/4	4357,03
	150	C+L	320	1	-	0/4	4/4	18000,00	1	0,00	4/4	0/4	9231,60
200	C+L+S	320	1	-	0/4	4/4	18000,00	1	-	0/4	4/4	18000,00	
Euro	10	C	80	1	0,00	4/4	0/4	38,67	1	0,00	4/4	0/4	10,11
	20	C	160	1028,5	0,00	4/4	0/4	2681,62	1	0,00	4/4	0/4	38,98
	30	C	160	921,75	0,00	4/4	0/4	5308,37	1	0,00	4/4	0/4	71,87
	40	C	240	2,5	6,87	0/4	2/4	18000,00	1	0,00	4/4	0/4	236,56
	50	C	240	1	-	0/4	4/4	18000,00	1	0,00	4/4	0/4	483,99
	100	C+L	320	1	-	0/4	4/4	18000,00	1	0,00	4/4	0/4	2682,91
	150	C+L	320	1	-	0/4	4/4	18000,00	1	0,00	4/4	0/4	8470,84
200	C+L+S	320	1	-	0/4	4/4	18000,00	1	0,00	4/4	0/4	11602,85	

The results clearly indicate that the Branch-and-Price outperforms the Branch-and-Cut in solving the RMSBA problem. Overall, the B&P demonstrates superior efficiency, successfully solving a higher percentage of instances to optimality. Specifically, the B&P solves approximately 89.45% of the instances to optimality, with an average computational time of 3837.93 seconds across all instances (including those not solved to optimality). In contrast, the B&C solves only 33.2% of the instances to optimality, with an average time of 13948.31 seconds (over all instances). Notably, 100% of the optimal solutions obtained by the B&P are found at the root node of the branching tree, compared to 87% for the B&C. In addition, the B&C was unable to provide at least a feasible solution for 67.19% of the instances, compared to only 8.6% when using the B&P. This highlights the B&P's ability to converge rapidly in many cases, often solving problems without extensive branching. Moreover, we observe that for large demand sets (i.e., when $|K| \geq 100$), the B&P maintains its effectiveness, solving 71.88% of these instances to optimality, whereas B&C fails to even find a feasible primal solution for all these instances. Additionally, while the B&P generally performs well, it occasionally encounters difficulties in providing feasible solutions for 22.92% of these large-demand instances. Furthermore, the fact that many solutions are obtained at the root node indicates that the B&P can effectively exploit the problem structure, reducing the need for extensive branching. However, this should be further demonstrated using larger graphs and demand sets. In addition, certain enhancement techniques, such as primal heuristics and additional valid inequalities to obtain tighter bounds, can be further utilized to enhance the performance of the B&C and B&P algorithms, especially for large-scale instances.

6 Conclusion and Future Works

In this study, we proposed a combinatorial optimization framework for solving the RMSBA problem in multi-band EONs, integrating key aspects such as security, resilience, energy efficiency, and cost-effective routing. Our approach employed both Branch-and-Cut and Branch-and-Price algorithms to solve the RMSBA problem. Numerical experiments demonstrated that the B&P algorithm outperforms the B&C algorithm in terms of solution quality and computational efficiency for all tested instances. However, the results also revealed limitations of the B&P approach when applied to larger instances, highlighting the need to integrate cutting-plane techniques and primal heuristics to further improve performance.

Future research could explore machine learning techniques to improve branching, column generation, cut selection, and parameter tuning, providing promising directions for more efficient solutions.

References

- [1] Marcelo Bianchetti. 2020. RSA instances. <https://github.com/exactasmache/RSAinstances>. Accessed: 2024-04-27.
- [2] Marcelo Bianchetti and Javier Marenco. 2025. The Routing and Spectrum Allocation Problem: A Combinatorial Optimization Survey. *Operations Research Forum* 6, 3 (2025), 95.
- [3] Cao Chen, Shilin Xiao, Fen Zhou, and Massimo Tornatore. 2024. Throughput Maximization in Multi-Band Optical Networks with Column Generation. In *ICC 2024 - IEEE International Conference on Communications*. 3034–3039.
- [4] Ibrahima Diarrassouba and Youssef Hadhbi. 2022. The Constrained-Routing and Spectrum Assignment Problem: Valid Inequalities and Branch-and-Cut Algorithm. In *Combinatorial Optimization - 7th International Symposium, ISCO 2022, Virtual Event, May 18–20, 2022, Revised Selected Papers (Lecture Notes in Computer Science, Vol. 13526)*, Ivana Ljubic, Francisco Barahona, Santanu S. Dey, and Ali Ridha Mahjoub (Eds.). Springer, 35–47.
- [5] Ibrahima Diarrassouba, Youssef Hadhbi, and Ali Ridha Mahjoub. 2022. The Constrained-Routing and Spectrum Assignment Problem: Extended Formulation and Branch-and-Cut-and-Price Algorithm. In *8th International Conference on Control, Decision and Information Technologies, CoDIT 2022, Istanbul, Turkey, May 17–20, 2022*. IEEE, 926–931.
- [6] Ibrahima Diarrassouba, Youssef Hadhbi, and Ali Ridha Mahjoub. 2024. Branch-and-cut-and-price algorithm for the constrained-routing and spectrum assignment problem. *J. Comb. Optim.* 47, 4 (2024), 56.
- [7] José Roberto do Nascimento Arcanjo, Eloisa Bento Sarmento, and Helder Alves Pereira. 2024. Analysis of the impact of different node and link architectures on the performance of multiband elastic optical networks. *Optical Fiber Technology* 88 (2024), 103956.
- [8] Moshe Dror. 1994. Note on the Complexity of the Shortest Path Models for Column Generation in VRPTW. *Operations Research* 42, 5 (1994), 977–978.
- [9] Mohammad Eskandarinia, Farhad Arpanaei, Hamzeh Beyranvand, Hami Rabani, Óscar González de Dios, Juan Pedro Fernández-Palacios, David Larrabeiti, and José Alberto Hernández. 2024. Maximizing Cost and Energy Savings in Multi-Band EONs through QoT-Driven Service Deployment. In *2024 IEEE International Mediterranean Conference on Communications and Networking*. 501–506.
- [10] Gerald Gamrath, Daniel Anderson, Ksenia Bestuzheva, Wei-Kun Chen, Leon Eifler, Maxime Gasse, and et al. 2024. The SCIP Optimization Suite 7.0. arXiv:2402.17702 [math.OC]
- [11] Andrew V. Goldberg and Robert E. Tarjan. 1988. A new approach to the maximum-flow problem. *J. ACM* 35, 4 (Oct. 1988), 921–940.
- [12] Youssef Hadhbi, Hervé Kerivin, and Annegret K. Wagler. 2019. A novel integer linear programming model for routing and spectrum assignment in optical networks. In *Proceedings of the 2019 Federated Conference on Computer Science and Information Systems, FedCSIS 2019, Leipzig, Germany, September 1–4, 2019*, Maria Ganzha, Leszek A. Maciaszek, and Marcin Paprzycki (Eds.), Vol. 18. 127–134.
- [13] Soheil Hosseini, Ignacio de Miguel, Noemi Merayo, Óscar González de Dios, and Ramón J. Durán Barroso. 2022. Survivability against Amplifier Failures in Multi-band Elastic Optical Networks. *2022 Asia Communications and Photonics Conference (ACP)* (2022), 1299–1302.
- [14] Rana Kumar Jana, Bijoy Chand Chatterjee, Abhishek Pratap Singh, Anand Srivastava, Biswanath Mukherjee, Andrew Lord, and Abhijit Mitra. 2022. Quality-aware resource provisioning for multiband elastic optical networks: a deep-learning-assisted approach. *Journal of Optical Communications and Networking* 14, 11 (2022), 882–893.
- [15] Nicolas Jara, Jorge Bermudez, Patricia Morales, Hermann Pempelfort, Ricardo Olivares, and Ariel Leiva. 2025. Multiband Elastic Optical Networks: Comprehensive Insights into Band Resource Management. In *2025 International Conference on Optical Network Design and Modeling (ONDM)*. 1–6.
- [16] Kaiwen Liu, Chenyu You, Shan Yin, Xiaodong Liu, Mengru Cai, and Shanguo Huang. 2024. Routing, Modulation Level and Spectrum Assignment Considering Energy Consumption in C+L-Bands Optical Network. In *2024 22nd International Conference on Optical Communications and Networks (ICOCN)*. 1–3.
- [17] Mahdieh Mehrabi, Hamzeh Beyranvand, and Mohammad Javad Emadi. 2021. Multi-Band Elastic Optical Networks: Inter-Channel Stimulated Raman Scattering-Aware Routing, Modulation Level and Spectrum Assignment. *Journal of Lightwave Technology* 39, 11 (2021), 3360–3370.
- [18] Stefan Nickel, Claudius Steinhardt, Hans Schlenker, and Wolfgang Burkart. 2022. *IBM ILOG CPLEX Optimization Studio—A primer*. Springer Berlin Heidelberg, Berlin, Heidelberg, 9–21.
- [19] Sebastian Orłowski, Roland Wessäly, Michal Pióro, and Artur Tomaszewski. 2010. SNDlib 1.0 - Survivable Network Design Library. *Networks* 55, 3 (2010), 276–286.
- [20] Daisuke Saito, Yojiro Mori, Kohei Hosokawa, Shigeyuki Yanagimachi, and Hiroshi Hasegawa. 2024. Cost-Effective Capacity Enhancement of Survivable Optical Networks by Supplemental Band Expansion and Backup Resource Sharing. *2024 Optical Fiber Communications Conference and Exhibition (OFC)* (2024), 1–3.
- [21] Amit Khanjan Sarma, Sanjib K. Deka, and Nityananda Sarma. 2025. Survivable Elastic Optical Network: A survey of failure scenarios and solutions. *Optical Switching and Networking* 58 (2025), 100823.
- [22] Giannis Savva, Konstantinos Manousakis, and Georgios Ellinas. 2018. Spread Spectrum over OFDM for Enhanced Security in Elastic Optical Networks. In *2018 Photonics in Switching and Computing (PSC)*. 1–3.
- [23] Anjali Sharma, Christofer Vasquez, and Carmen Mas Machuca. 2025. Routing, Band, Modulation and Spectrum Assignment with Dedicated Protection in Multiband- Elastic Optical Networks. In *International Conference on ONDM, 2025, Pisa, Italy, May 6–9, 2025*, Luca Valcarengi, Andrea Sgambelluri, Carmen Mas Machuca, and Raul Muñoz (Eds.). IEEE, 1–6.
- [24] Sahar Talebi, Furqan Alam, Iyad Katib, Mohamed Khamis, Reda Salama, and George N. Rouskas. 2014. Spectrum management techniques for elastic optical networks: A survey. *Optical Switching and Networking* 13 (2014), 34–48.
- [25] Qian Wu, Jiading Wang, Sibao Chen, and Atsushi Kanai. 2022. Resource allocation problem in multi-band space-division multiplexing elastic optical networks. In *2022 18th International Conference on Computational Intelligence and Security (CIS)*. 225–228.